1 Mechanics of the cytoskeleton

We have previously learned about the mechanics of biopolymers. We now have the proper foundation to learn about the mechanics of networks of biopolymers: in other words, the cytoskeleton! The microstructure of the cytoskeleton (e.g., how the biopolymers are oriented with respect to one another, the number of filaments per unit volume, how they are cross-linked, etc.) can vary dramatically from cell to cell. It can also vary substantially within different locations of individual cells. The mechanics of the cytoskeleton are dependent on the mechanical behavior of the individual biopolymers making up the cytoskeleton (which we learned about in the last section), as well as how these biopolymers are organized into a network (i.e., microstructure). The goals of this next section are to show some examples of (1) the mechanical implications of different types of cytoskeletal microstructure, and (2) how to calculate mechanical properties for a given cytoskeletal network knowing only the mechanical behavior and microstructural organization of the individual polymers.

1.1 Mechanics of filopodia

Filopodia are dynamic, cross-linked bundles of actin filaments at the leading edge of crawling cells. Morphologically, they resemble little fingers, and they are thought to act as "feelers" as the cell crawls. These bundles of actin quickly grow out from the leading edge, pushing out the membrane (typically on the order of $\sim$0.1 μm/s to form rod-like structures, and then retract (total time for extension and retraction is on the order of $\sim$100 s). The filopodia are on the order of $\sim$0.2 μm in diameter and 1$\sim$5 μm in length. Within a single filopodium, 20$\sim$30 actin filaments are aligned in parallel [5] with their barbed ends facing the membrane, and cross-linked by a protein called fascin. At the ends of the filaments within the filopodia is a protein called capping protein, aptly named since they cap the actin filaments to prevent further growth.

The way in which cells are able to form filopodia and regulate their structure is still an active area of investigation. Indeed, even fundamental questions about their structure, such as how densely cross-linked the actin filaments are, is still under investigation. The question is whether mechanics can tell us anything about their structure? In addition, and perhaps more importantly, are mechanics involved in regulating their structure?

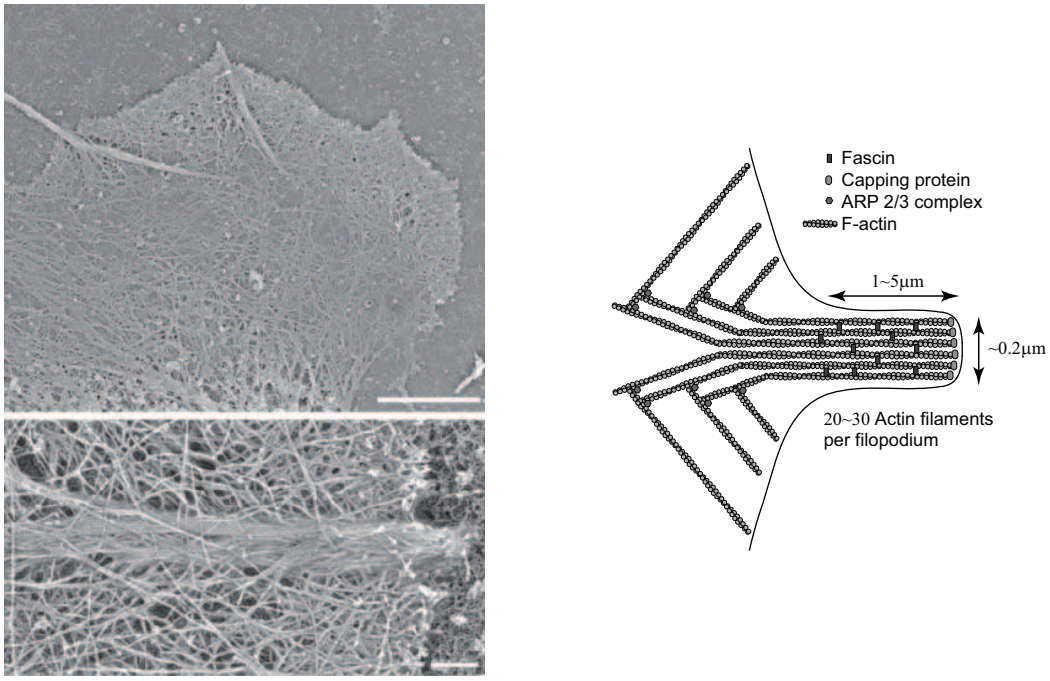

Figure 1.1: Left,top: Electron micrograph of the actin cytoskeleton within a lamellopodium of a cell [4]. A dense network of actin filaments can be seen. Several filopodia can be seen protruding from the edge. Left, bottom: Close up of a filopodium [4]. The aligned bundle of actin filaments can be seen. Right: Schematic of several important proteins within filopodium. Note that the actin filaments within each filopodium are bundled together by the cross-linking protein fascin.

We will attempt to try to answer some of these questions here by finding the maximum length filopodia can be before they will buckle, assuming (1) no cross-linking is present, or (2) a high degree of cross-linking. We know that the persistence length of F-actin is on the order of $\sim$10 μm, while the filopodia are on the order of $\sim$1 μm in length. Since the persistence length of actin is an order of magnitude larger than the average length of the filaments within the filopodia, we neglect any entropic contributions to their mechanical behavior, and analyze the filaments as beams. For more details, see [5], from which the approach here was followed.

1.1.1 Buckling force

Before we begin our analysis, we first need a relation between the buckling force of a beam, and its geometry and material properties. Consider a beam of length L with one end fixed, and with an axial force F applied at the free end (see Figure 1.1.1). The beam will buckle if F exceeds the buckling force,

$$F_{buckle} = \frac{\pi^2 EI}{4L^2} \tag{1.1.1}$$

where E is the Youngs modulus of the beam, and I is the moment of inertia.

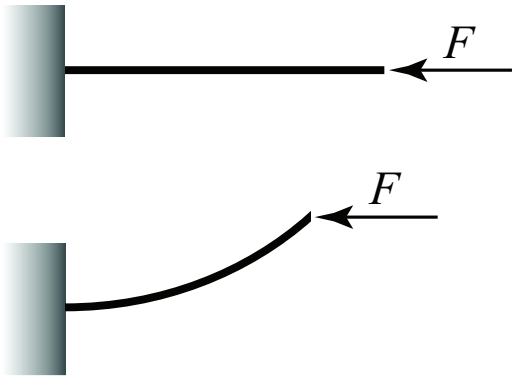

Figure 1.2: A beam with one end fixed and a force F applied at the free end will buckle if F is large enough.

1.1.2 Membrane force

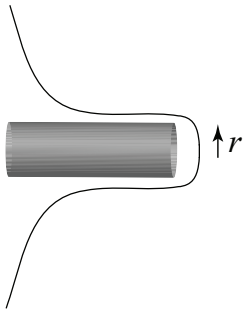

Figure 1.3: The force exerted on a cylindrical protrusion by a membrane is proportional radius of the cylinder.

Next, we need an estimation of the force that the membrane exerts on the actin bundle at the ends of the filopodia. If we idealize the actin bundle as a cylinder of radius r, then we need to find the force F_{mem} exerted on this cylinder by the membrane. A simple approximation by can be made by making an imaginary cut through the cylinder and membrane. The resultant force of the membrane is

equal to the product of the surface tension N of the membrane and the circumference of the cylinder:

$$F_{mem} = 2\pi r N. \tag{1.1.2}$$

For neutrophils, the surface tension as measured through micropipette aspiration has been found to be approximately 35 pN/μm [3], resulting in a force of 22 pN for a filopodium 100 nm in radius. However, this force does not take into account membrane bending and breaking of membrane-cortex links, both of which will contribute resistance to protrusion [6]. Experimentally, $\sim$ 50 pN of force has been found to be necessary to form filopodium-like membrane tethers within neutrophils citeshao96. This likely is a more accurate estimation of F_{mem}, and so we will assume $F_{mem} = 50$ pN.

1.1.3 Maximum length before buckling: no cross-linking

We will now calculate the maximum filopodium length before buckling occurs, assuming no cross-linking. Assume that there are $n = 30$ actin filaments within the bundle, with each filament having a radius of $r_{actin} = 3.5$ nm and Youngs modulus of $E_{actin} = 1.9$ GPa. Each filament will feel a force of F_{mem}/n, and so the maximum filopodium length before buckling occurs is

$$\begin{aligned} L_{nocl} &= \sqrt{\frac{\pi^2 E_{actin} I_{actin}}{4F_{buckle}}} \\ &= \sqrt{\frac{\pi^2 E_{actin} \frac{\pi r_{actin}^4}{4}}{4\frac{F_{mem}}{n}}}. \end{aligned} \tag{1.1.3}$$

Plugging in the appropriate values gives $L_{nocl} = 0.57$ μm. Therefore, for a filopodium containing 30 actin filaments that are not cross-linked, it can only be 0.57 μm long before it will buckle. This is much shorter than the 1$\sim$5 μm long filopodia observed in vivo. Lets see what happens if we now take cross-linking into account.

1.1.4 Maximum length before buckling: with cross-linking

In order to investigate the effect of cross-linking, we assume that the bundle is tightly cross-linked such that the bundle acts as a single filament of effective radius r_{bundle}. To calculate this radius, we know that for a bundle of n filaments, the total cross-sectional area of F-actin is

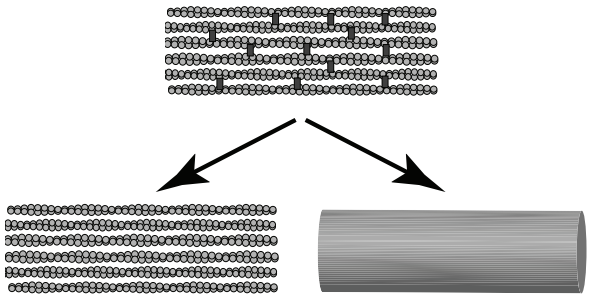

Figure 1.4: Two different approximations for analyzing the filopodium. One is where we assume no cross-linking. The second is where we assume that the bundle is so tightly cross-linked, it behaves as single, large cylinder.

$$n\pi r_{actin}^2 = \pi(\sqrt{n}r_{actin})^2. \tag{1.1.4}$$

The term in parenthesis on the righthand side of 1.1.4 gives the radius of a cylinder with the same cross sectional area of n actin filaments, which is the effective radius of the bundle:

$$r_{bundle} = \sqrt{n}r_{actin}. \tag{1.1.5}$$

Now, the moment of inertia of the bundle becomes

$$\begin{aligned} I_{bundle} &= \frac{\pi r_{bundle}^4}{4} \\ &= \frac{\pi(\sqrt{n}r_{actin})^4}{4}. \end{aligned} \tag{1.1.6}$$

Finally, assuming $F_{buckle} = F_{mem}$, then

$$L_{cl} = \sqrt{\frac{\pi^2 E_{actin} I_{bundle}}{4F_{buckle}}} = \sqrt{\frac{\pi^2 E_{actin} \frac{\pi(\sqrt{n} r_{actin})^4}{4}}{4F_{mem}}}. \quad (1.1.7)$$

Substituting the appropriate values gives a value of $L_{cl} = 3.2$ μm. In other words, for a highly cross-linked filopodium, it can be 3.2 μm long before buckling occurs. Comparing Equations 1.1.3 and 1.1.7, we find that the ratio of $L_{cl}/L_{nocl} = \sqrt{n}$. The more filaments that are in each filopodium, the more pronounced the difference in the buckling lengths between the cross-linked and uncross-linked filopodia.

What can be learned from our analysis? We have already learned that filopodia 1$\sim$5 μm are commonly observed in vivo. Our analysis showed that without cross-linking, filopodia will buckle before they are able to reach these lengths. However, if they are highly cross-linked, they are much more stable mechanically, and won't until they are several microns long. This suggests that there is a high degree of cross-linking within filopodia [5]. Finally, our analysis also suggests the possibility that filopodia length is governed by mechanics, in they they are not longer since this will cause them to buckle! Although this is purely speculation, the mechanical regulation of cytoskeletal structure within subcellular structures such as filopodia continues to be an active area of research.

1.2 Mechanics of the red blood cell cytoskeleton

The mechanical behavior of red blood cells is very important for their function. For example, in order to deliver oxygen to different parts of the body, they must be able to squeeze through tiny capillaries (many of which have diameters that are smaller than the cells themselves), and then return to their original shape upon exiting the capillaries.

One of the main mechanical constiuents of red blood cells is the cytoskeleton. The role of its distinct and highly structured architecture in the function of red blood cells continues to be an active area of research. In red blood cells, the cytoskeletal network is bound to the membrane in a two-dimensional network. The main constiuent of the network is a polymer called spectrin. The spectrin polymers are bound together at distinct vertices, or "junctions". At each vertex is a junctional complex consisting of several proteins (including F-actin) that serve to cross-link the spectrin polymers together, as well as anchor the cytoskeletal network to the

membrane. There are also protein complexes along the length of the spectrin polymer that anchor it directly to the membrane. The red blood cell cytoskeleton is highly structured. At each junction, six spectrin polymers are commonly observed radiating from each junction. This is termed sixfold connectivity. Fourfold connectivity, or four spectrin polymers radiating from each junction, has also been observed. A question one can ask is what are the structural and functional implications of these different connectivities?

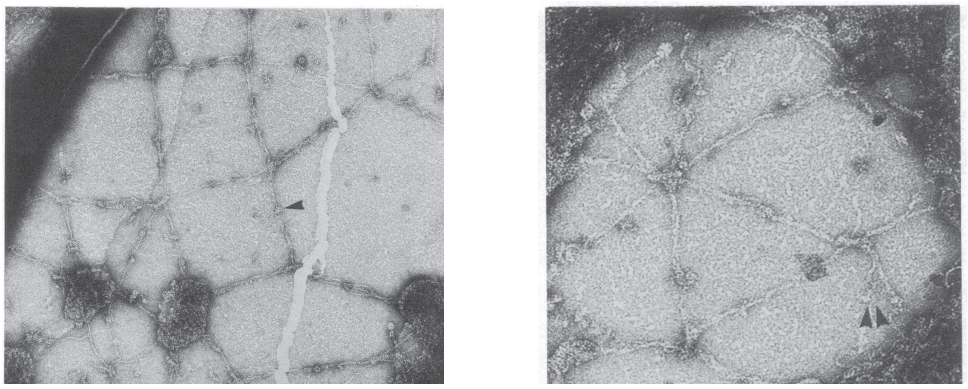

Figure 1.5: Electron micrographs of the red blood cell cytoskeleton with different connectivities. Adapted from [2]

As the analytical and numerical tools for analyzing the mechanics of the red blood cell cytoskeleton become more sophisticated, the impact of such distinct microstructures on the mechanical behavior of red blood cells are becoming more well understood. However, we can also learn a lot from simple analyses as well. We demonstrate here a procedure for calculating the mechanical properties of the red blood cell cytoskeleton from the mechanical behavior of its polymers and its microstructure. By seeing how these properties change with different microstructures, we also propose why red blood cells sixfold connectivity may be advantageous for red blood cells for their function. For more detailed analyses, see [1], from which the approach here was followed.

1.2.1 Shear modulus and strain energy density

We know that the shear modulus G gives the stiffness of an object in resisting shear, and it relates the shear stress τ that results from a given (engineering) shear strain γ,

$$\tau = G\gamma. \tag{1.2.1}$$

Consider a block with length l, height h, depth d, and shear modulus G. We shear the block by displacing the top surface by a small amount δ, which results in the sides of the block making an angle of γ with an imaginary vertical line. We know that

$$\begin{aligned} \gamma &= \frac{\partial u}{\partial y} + \frac{\partial v}{\partial x} \\ &= \frac{\delta}{h} \\ &= \tan\gamma \\ &\approx \gamma \end{aligned} \tag{1.2.2}$$

where in the last line the approximation $\tan\gamma \approx \gamma$ is valid for small γ. In other words, the shear strain is simply the angle with the vertical, γ. Since it takes work to shear the block, it must undergo a change in strain energy ΔW. Its strain energy per unit undeformed volume, called the strain energy density, is

$$\Delta w_v = \frac{\Delta W}{V}, \tag{1.2.3}$$

where $V = lwh$ is the undeformed volume of the block. Since we know the shear modulus and shear strain, we can compute its strain energy density from these two quantities as

$$\Delta w_v = \frac{1}{2} G\gamma^2. \tag{1.2.4}$$

Alternatively, lets say that we know the strain energy density of the object for a certain shear strain γ, and want to know its shear modulus. Upon inspection of 1.2.4, we find that we can calculate the shear modulus by differentiating its strain energy density:

$$\begin{aligned}\frac{\partial^2 \Delta w_v}{\partial \gamma^2} &= \frac{\partial^2 \frac{1}{2} G\gamma^2}{\partial \gamma^2} \\ &= \frac{\partial G\gamma}{\partial \gamma} \\ &= G. \end{aligned} \tag{1.2.5}$$

Therefore, if we know the change in strain energy ΔW of the block as it undergoes shear strain γ, we can find its shear modulus G by simply dividing by the undeformed volume to get Δw_v, and differentiating twice with respect γ!

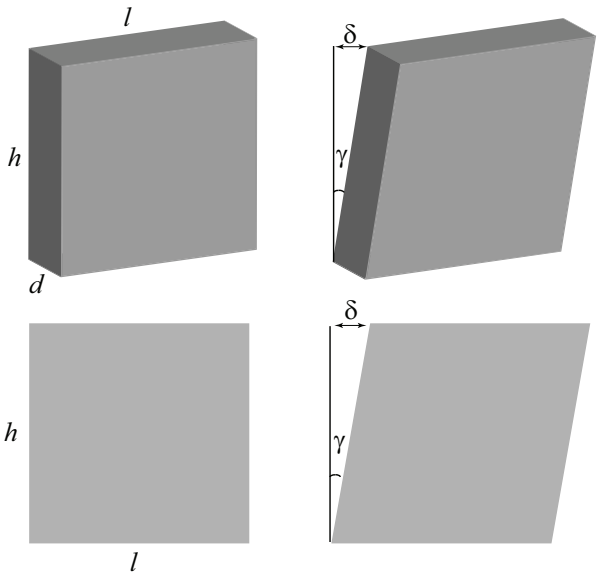

Figure 1.6: (Top) A block undergoing shear strain γ by displacing the top surface by a small amount δ. (Bottom) An equivalent two-dimensional block undergoing shear.

Now, consider the case where the block is "thin" (i.e., it has a very small depth d). For thin structures, we usually are not interested in how quantities such as stress and strain change with depth. It is mathematically convenient to treat them as "two-dimensional" structures by integrating out the depth of the block. For example, instead of a shear stress (with units of force per area), we can define a shear force per unit length N_s such that

$$N_s = \tau d \tag{1.2.6}$$

where we have assumed that the shear stress is constant through the depth. This can be related to the shear strain analagous to 1.2.1 as

$$N_s = K_s \gamma \tag{1.2.7}$$

where K_s is the shear modulus,

$$K_s = Gd. \tag{1.2.8}$$

Similarly, analagous to Equations 1.2.3, 1.2.4, and 1.2.5, the strain energy per unit area (instead of volume) $w_a = \Delta W/A$ can be calculated from the shear modulus and shear strain as

$$\Delta w_a = \frac{1}{2} K_s \gamma^2, \tag{1.2.9}$$

and the strain energy density can be differentiated to obtain the shear modulus as

$$\frac{\partial^2 \Delta w_a}{\partial \gamma^2} = K_s. \tag{1.2.10}$$

Using these relations, we will now calculate K_s for the red blood cell cytoskeleton assuming sixfold or fourfold connectivity. Our strategy is to find the total change in strain energy ΔW for a given shear strain γ, divide by the undeformed area to obtain Δw_a, and finally find K_s using 1.2.10.

1.2.2 Sixfold connectivity

In order to analyze the cytoskeletal network, we first need to determine how to model the polymers and microstructure. In vivo, the spectrin polymers have a countour length of $L = 200$ nm, and a persistence length of $l_p = 15$ nm. The junctions are separated by a distance of 75 nm. Since $l_p << L$ and the spectrin polymers are not fully stretched out (i.e., $R < L$), then we assume that the spectrin polymers behaves as entropic springs. In this case, we can analyze the cytoskeleton as a network of springs with spring constant $k_{sp} = (3kT)/(Lb)$, connected at the junctions by freely rotating cross-links. In this case, we can find the strain energy by finding how much the springs deform under shear strain γ.
In order to simplify our analysis, we can analyze a unit cell of the network instead of an entire network. Consider a sixfold network of springs with constant k_{sp}. If we use an equilateral triangle of springs with constant k_{sp} as the unit cell of the

network, then we can see in Figure 1.2.2 that each pair of neighboring triangles contributes a spring between each pair of junctions, resulting in two springs of stiffness k_{sp} (or equivalently, a single spring of stiffness $2k_{sp}$) between each pair of junctions. We can correct this by making the stiffness of our springs in our equilateral triange equal to $k_{sp}/2$.

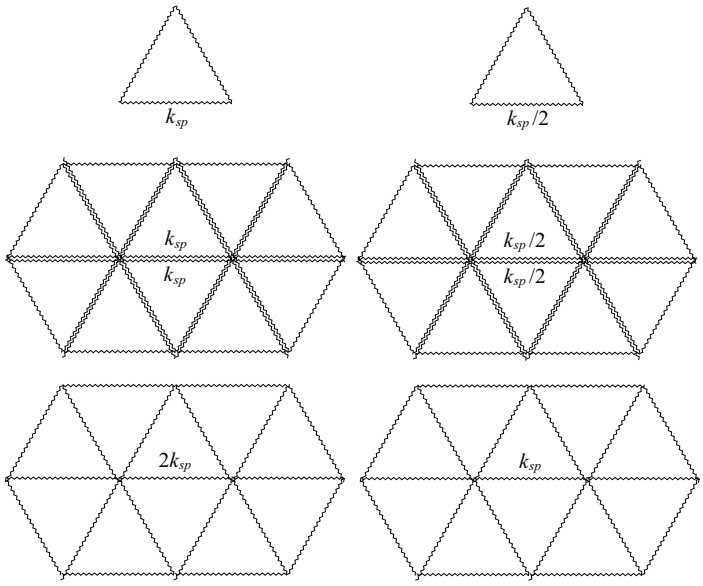

Figure 1.7: An equilateral triangle of springs with constant k_{sp} is the unit cell for a sixfold network of springs with constant $2k_{sp}$ (left). In contrast, an equilateral triangle of springs with constant $k_{sp}/2$ is the unit cell for a sixfold network of springs with constant k_{sp} (right), which is the desired result.

Now, consider an equilateral triangle of springs, each with length R_0. The triangle has a height of

$$\begin{aligned} h &= \sqrt{R_0^2 - \left(\frac{R_0}{2}\right)^2} \\ &= \frac{\sqrt{3}R_0}{2}. \end{aligned} \tag{1.2.11}$$

If we now displace the top vertex by a small amount δ such that the triangle undergoes shear strain γ, then

$$\begin{aligned} \tan\gamma &= \frac{\delta}{h} \\ &= \frac{2\delta}{\sqrt{3}R_0}. \end{aligned} \tag{1.2.12}$$

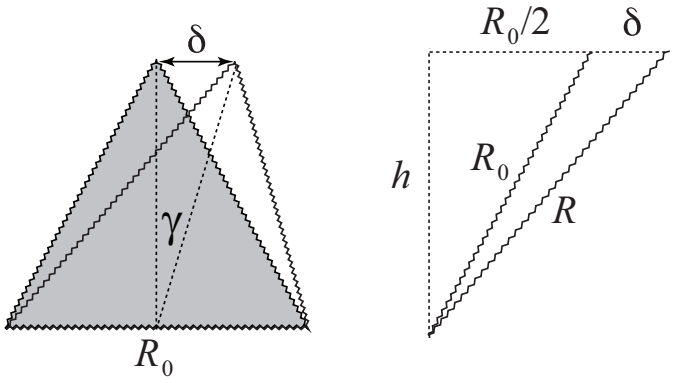

Figure 1.8: An equilateral triangle of springs undergoing shear strain γ by displacing the top surface by a small amount δ.

But $\tan\gamma \approx \gamma$ for small δ, so 1.2.12 can be rewritten as

$$\delta = \frac{\sqrt{3}R_0\gamma}{2}. \tag{1.2.13}$$

Under this deformation, the left and right diagonal springs lengthen and shorten, respectively, while the bottom spring does not change length. The deformed length R of the left diagonal spring can be found from geometry:

$$\begin{aligned} R &= \sqrt{h^2 + \left(\frac{R_0}{2} + \delta\right)^2} \\ &= \sqrt{\left(\frac{\sqrt{3}R_0}{2}\right)^2 + \left(\frac{R_0}{2} + \delta\right)^2} \\ &= \sqrt{R_0^2 + R_0\delta + \delta^2} \\ &= \sqrt{R_0^2 + \frac{R_0^2\delta}{R_0} + \frac{R_0^2\delta^2}{R_0^2}} \\ &= R_0\sqrt{\frac{\delta}{R_0} + \frac{\delta^2}{R_0^2}}. \end{aligned} \tag{1.2.14}$$

Since δ is small, we ignore higher order terms in δ, and 1.2.14 becomes

$$R \approx R_0\sqrt{1 + \frac{\delta}{R_0}}. \tag{1.2.15}$$

We can simplify 1.2.17 even further by noticing that

$$\begin{aligned}\left(1+\frac{\delta}{2R_0}\right)^2 &= 1+\frac{\delta}{R_0}+\frac{\delta^2}{4R_0^2} \\ &\approx 1+\frac{\delta}{R_0}\end{aligned} \tag{1.2.16}$$

if we ignore higher order terms. Thus, 1.2.17 can be rewritten as

$$\begin{aligned}R &\approx R_0\sqrt{\left(1+\frac{\delta}{2R_0}\right)^2} \\ &\approx R_0+\frac{\delta}{2}.\end{aligned} \tag{1.2.17}$$

This implies that the left diagonal spring increases in length by $\delta/2$ to first order. It can be shown similarly that the right diagonal spring shortens by the same amount. We know that the change in strain energy for a spring with constant k_{sp}, original length R_0 and new length R is

$$\Delta W_{sp} = \frac{1}{2}k_{sp}(R-R_0)^2. \tag{1.2.18}$$

The total change in strain energy is the sum of the change in strain energy for all three springs. Assuming a spring constant of $k_{sp}/2$, this expression becomes

$$\begin{aligned}\Delta W &= \Delta W_{sp}^{left}+\Delta W_{sp}^{right}+\Delta W_{sp}^{bottom} \\ &= \frac{1}{2}\left(\frac{k_{sp}}{2}\right)((R_0+\delta/2)-R_0)^2+\frac{1}{2}\left(\frac{k_{sp}}{2}\right)((R_0-\delta/2)-R_0)^2+0 \\ &= \frac{k_{sp}\delta^2}{8}.\end{aligned} \tag{1.2.19}$$

The strain energy density can be found by dividing ΔW by the undeformed area of the triangle:

$$\begin{aligned}\Delta w_a &= \frac{\Delta W}{A} \\ &= \frac{\frac{k_{sp}\delta^2}{8}}{\frac{1}{2}R_0 h} \\ &= \frac{\frac{k_{sp}\delta^2}{8}}{\frac{1}{2}R_0\frac{\sqrt{3}R_0}{2}} \\ &= \frac{k_{sp}\delta^2}{2\sqrt{3}R_0^2}. \end{aligned} \tag{1.2.20}$$

We can write the strain energy density in terms of γ by substituting 1.2.13 into 1.2.20, which becomes

$$\Delta w_a = \frac{\sqrt{3}k_{sp}\gamma^2}{8}. \tag{1.2.21}$$

Finally, the shear modulus of the network K_s is

$$\begin{aligned}K_s &= \frac{\partial^2 \Delta w_a}{\partial \gamma^2} \\ &= \frac{\sqrt{3}k_{sp}}{4}. \end{aligned} \tag{1.2.22}$$

How does our prediction compare to experiments? Substituting $b = 30$ nm, $T = 300$ K, $L = 200$ nm gives $K_s = 0.9$ μN/m. Experimental measurements of K_s of red blood cell cytoskeletons in which the membrane was removed showed average values of the shear modulus to be $K_s = 2.4$ μN/m. This is roughly twice our predicted value but still in excellent agreement. What are some sources of error? One may be our approximation of spectrin as a Gaussian chain. Remember that when R approaches L, the stiffness of a real chain will increase, while the stiffness of a Gaussian chain will not. Thus, the Gaussian approximation is best when $L >> R$, whereas for the red blood cell cytoskeleton, L is only a little more than twice that of R.

1.2.3 Fourfold connectivity

We will now calculate K_s for a fourfold network. Here, our unit cell is a square lattice of springs, each with spring constant $k_{sp}/2$ and undeformed length R_0. If

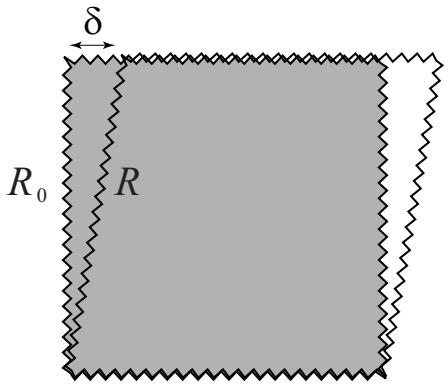

Figure 1.9: A square network of springs undergoing shear by displacing the top surface by a small amount δ.

we displace the top surface of the square by a small amount δ, then the top and bottom springs do not change length, and the deformed lengths of the left and right springs are

$$\begin{aligned} R &= \sqrt{R_0^2 + \delta^2} \\ &\approx R_0^2 \end{aligned} \tag{1.2.23}$$

if we ignore higher order terms. What this means is that, to first order, the left and right springs do not change length! This implies that the change in strain energy will be zero, and so $K_s = 0$! Intuitively, this makes sense, since the stiffness in shear of our networks of springs arises due to the springs changing in length. However, if the springs do not change length, then the network can not resist shear, and so it has no stiffness in shear. This suggests that sixfold connectivity is highly advantageous for red blood cells compared to fourfold connectivity, since sixfold connectivity allows resistance to shear! Such resistance may be important in allowing red blood cells to squeeze through tiny capillaries, and return back to their original shape.

Bibliography

[1] BOAL, D. [2002]. *Mechanics of the Cell*. Cambridge University Press, Cambridge.

[2] BYERS, T. J., & D. BRANTON [1985]. 'Visualization of the protein associations in the erythrocyte membrane skeleton,' *Proc. Natl. Acad. Sci.*, **82**, pp. 6153–6157.

[3] EVANS, E. & A. YEUNG [1989]. 'Apparent viscosity and cortical tension of blood granulocytes determined by micropipet aspiration.' *Biophys J*, **56**, pp. 151–160.

[4] MEJILLANO, M. R., S. KOJIMA, D. A. APPLEWHITE, F. B. GERTLER, T. M. SVITKINA, & G. B. BORISY [2004]. 'Lamellipodial versus filopodial mode of the actin nanomachinery: pivotal role of the filament barbed end.' *Cell*, **118**, pp. 363–373.

[5] MOGILNER, A. & B. RUBINSTEIN [2005]. 'The physics of filopodial protrusion.' *Biophys. J.*, **89**, pp. 782–795.

[6] SHAO, E. Y., R. M. HOCHMUTH [1996]. 'Micropipette suction for measuring piconewton forces of adhesion and tether formation from neutrophil membranes.' *Biophys. J.*, **71**, pp. 2892–2901.